Check for updates

Allergy

WILEY | EAACI

ORIGINAL ARTICLE OPEN ACCESS

Multi-Omics Analysis Reveals Vitamin D Metabolism, Hyper-IgE Genes, and Epithelial Barrier Dysfunction in Hazelnut Allergy

Alexander C. S. N. Jeanrenaud[1,2,3] | Aleix Arnau-Soler[1,2,3,4] | Ahla Ghauri[1,2,3] | Ingo Marenholz[1,2,3] | Philipp Mertins[1,4,5] | Matthias Ziehm[1,5] | Kirsten Beyer[3,4,6] | Margitta Worm[3,7] | Young-Ae Lee[1,2,3,4]

[1]Max Delbrück Center for Molecular Medicine, Helmholtz Association, Berlin, Germany | [2]Clinic for Pediatric Allergy, Experimental and Clinical Research Center, Charité-Universitätsmedizin, Berlin, Germany | [3]KFO339, Food@, Berlin, Germany | [4]German Center for Child and Adolescent Health (DZKJ), partner site Berlin, Berlin, Germany | [5]Berlin Institute of Health, Berlin, Germany | [6]Department of Pediatric Respiratory Medicine, Immunology and Critical Care Medicine, Charité-Universitätsmedizin Berlin, Freie Universität Berlin and Humboldt-Universität zu Berlin, Berlin, Germany | [7]Division of Allergy and Immunology, Department of Dermatology, Venerology and Allergy, Charité-Universitätsmedizin Berlin, Freie Universität Berlin and Humboldt-Universität zu Berlin, Berlin, Germany

Correspondence: Young-Ae Lee (yo.lee@charite.de)

Received: 27 December 2025 | **Revised:** 22 July 2026 | **Accepted:** 17 September 2026

Keywords: epigenetics | food allergy | hazelnut | multi-omics

ABSTRACT

Background: Hazelnut allergy is a major cause of food-induced anaphylaxis yet remains poorly defined at the molecular level. We aimed to identify molecular differences between individuals with primary hazelnut allergy and nonallergic controls by investigating a comprehensive spectrum of omics profiles in immune cells.

Methods: We analysed DNA methylation, transcriptomic, and proteomic profiles in hazelnut-stimulated and unstimulated immune cells.

Results: Across analyses, we identified 87 differentially methylated signatures, 125 unique differentially expressed genes, and 11 unique differentially secreted proteins associated with hazelnut allergy. DNA methylation signatures were largely preserved irrespective of antigen stimulation, indicating stable epigenetic remodelling. Key findings implicated *ZNF341*, associated with a rare monogenic hyper-IgE syndrome, and *ARL2*, both linked to STAT3-mediated IgE dysregulation. We identified a hypermethylated region overlapping *TH2LCRR* in the cytokine gene cluster, suggesting an epigenetic mechanism contributing to IL-5 and IL-13 upregulation. Antigen stimulation was required to reveal hazelnut-specific transcriptional and proteomic signals. Integration of these data demonstrated that IL-5 expression could distinguish both groups. Moreover, integrated analysis of all multi-omics data revealed prominent innate immune activation programs involving antimicrobial, antiviral, and cytokine-mediated inflammatory responses. Finally, we identified signals in epithelial barrier genes of the gut and skin (*TRIM31*, *TRIM40*, *CDSN*), activation of the vitamin D pathway (*CYP27B1*, *IL32*), and nominated additional signals (*PHACTR1, MFHAS1, SPRED2, NSMCE1-DT*) for follow-up.

Abbreviations: BMIQ, Beta-MIxture Quantile dilation; CSF, colony-stimulating factors; DEG, differentially expressed gene; DEP, differentially expressed protein; DMP, differentially methylated probe; DMR, differentially methylated region; DMSO, dimethyl sulfoxide; eQTM, expression quantitative trait methylation; EWAS, epigenome-wide association study; FBS, foetal bovine serum; GSEA, Gene Set Enrichment Analysis; IDOL, Identifying Optimal Libraries; logFC/log2FC, log2 fold change; MOFA, Multi-Omics Factor Analysis; MSigDB, Molecular Signature Database; OFC, oral food challenge; PBMC, peripheral blood mononuclear cell; PCA, principle component analysis; PPI, protein–protein interaction; QC, quality control; RIN, RNA integrity number; RPM, revolutions per minute; SNP, single nucleotide polymorphism; SPT, skin prick test; ssNOOB, single-sample normal-exponential out-of-band; STAR, Spliced Transcripts Alignment to a Reference; TINA, tolerance induction through non-avoidance to prevent persistent food allergy.

This is an open access article under the terms of the Creative Commons Attribution License, which permits use, distribution and reproduction in any medium, provided the original work is properly cited.

© 2026 The Author(s). *Allergy* published by European Academy of Allergy and Clinical Immunology and John Wiley & Sons Ltd.

Conclusion: This study provides the first antigen-specific multi-omics characterization of hazelnut allergy, confirming coordinated alterations in type 2-immunity and uncovering novel links to monogenic hyper-IgE syndrome, innate inflammatory pathways, activation of vitamin-D pathways, and gut/skin barrier genes, yielding a catalogue of candidate biomarkers for mechanistic studies and prospective validation.

1 | Introduction

Food allergy is a significant and increasing public health concern [1, 2]. As the global burden of food allergy rises, there is a growing need to deepen our understanding of the biological mechanisms driving allergen immune responses. Among food allergies, those against tree nuts are especially concerning due to their severity and association with a reduced quality of life [3, 4]. Members of the tree nut family include hazelnut, walnut, almond, pecan nut, cashew, pistachio, and Brazil nut. Among these, hazelnut allergy is the most common tree nut allergy in Europe [4, 5], presenting with reactions ranging from mild to life-threatening, particularly among children [6–8]. Although hazelnut allergy generally manifests in childhood, it typically persists into adulthood, thereby contributing to long-term socioeconomic challenges [9].

Multi-omics studies have successfully identified several mechanisms underlying food allergies, but primarily focused on peanut allergy and peanut oral immunotherapy response [10–12]. Few studies have examined the genetic mechanisms underlying tree nut allergy [13–16]. A genome-wide association study identified a hazelnut-associated locus near *HLA-DPA1*, whereas another study characterized gene expression changes in the absence of antigen-specific immune cell activation [13, 17]. The role of epigenetics and proteomics in hazelnut allergy also remains unexamined. This highlights the need to further our understanding of hazelnut allergy from a multi-omics antigen-specific perspective.

In this study, we aimed to address these gaps by comparing multi-omics profiles of double-blind placebo-controlled oral food challenge-(OFC) confirmed hazelnut-allergic individuals against nonallergic controls. We integrate in parallel genome-wide methylation profiling, mRNA sequencing, and secreted inflammatory proteins captured from isolated immune cells after 48 h stimulation with hazelnut protein. Our findings provide insights into the mechanisms distinguishing hazelnut-allergic from nonallergic individuals and provide a foundation for further research to inform the development of targeted therapies and improve diagnostic accuracy for hazelnut-allergic individuals.

2 | Methods

Detailed methodology is provided in the Supporting Methods. Software packages and tools are listed in Table E1, and materials used are outlined in Table E2.

2.1 | Study Cohort

Study participants were recruited as part of the Tolerance Induction through Non-avoidance to prevent persistent food Allergy (TINA) trial [18]. This study was approved under trial Ethics No. EA2/033/19 and EA2/304/21; German Clinical Trials Register ID: DRKS00016764 (RCT) DRK S00020467 [18]. Hazelnut-allergic individuals ($n = 24$) were OFC confirmed and nonallergic individuals ($n = 109$ after QC) defined as having no history of food- or aero-allergies as well as negative skin prick tests. Sample demographics are shown in Table 1 and Table E3. Written informed consent was provided by all study participants or their caregivers. The participants of this study were not receiving any form of oral immunotherapy at the time of analysis. To assess whether clinical reactivity was associated with age in the allergic cohort, we tested for association between age and the maximum tolerated dose during OFC using Spearman's rank correlation test. To account for the small sample size and unequal sample distribution, we also categorized cases into age tertiles (3 groups) and used the Kruskal-Wallis rank sum test to evaluate differences in the maximum tolerated dose between groups (Figure E1).

2.2 | Hazelnut Extract Preparation

Hazelnut protein extract was prepared from roasted hazelnut (Seeberger, Kaufland). Stock protein concentration was 21.3 mg/mL (Pierce BCA assay). Endotoxin was removed using Pierce High-Capacity Endotoxin Removal Resin; diluted aliquots (2.51 mg/mL) had endotoxin levels of 0.484EU/mL. At a working concentration (100 μg/mL), endotoxin content was 0.02EU/mL, below the accepted FDA limit of 0.5EU/mL for medical devices [19].

2.3 | Cell Culture

Whole blood was collected into sodium heparin tubes, in allergic individuals before OFC and in nonallergic individuals during screening. Peripheral blood mononuclear cells (PBMCs) were isolated using SepMate tubes (STEMCELL Technologies GmbH, Germany) and BioColl density gradient centrifugation (Sigma-Aldrich Chemie GmbH, Germany) and cryopreserved. 2 million PBMCs were cultured for 48-h in the absence (quiescent) or presence (stimulated) of 100 μg/mL hazelnut protein extract in a total of 500 μL media. In total, we studied 24 hazelnut-allergic and 111 nonallergic individuals; following cell culture and antigen stimulation, this yielded 22 quiescent and 24 stimulated (46 total) samples from the allergic individuals, and 111 quiescent and 111 stimulated (222 total) samples from the nonallergic individuals. Two individuals (four samples) were removed from the nonallergic group following quality control (QC; $n = 218$ total; Figure E1).

2.4 | DNA, RNA, and Protein Isolation

Following 48-h cell culture, DNA and RNA were co-extracted from cell pellets using a combination of Qiagen AllPrep DNA/

TABLE 1 | Characteristics of the study participants.

Hazelnut cohort characteristics	Hazelnut allergic ($N=24$)[a]	Nonallergic ($N=109$)[a]	p[b]
Age at blood collection (years)	8 (5, 24)	26 (22, 30)	<0.001
Sex (F)	11 (46%)	70 (64%)	0.095
History of asthma	8 (33%)	2 (1.8%)	<0.001
History of Eczema	19 (79%)	2 (1.8%)	<0.001
Allergic Rhinoconjunctivitis	12 (50%)	0 (0%)	<0.001
SPT hazelnut roasted (mm)	6.00 (3.00, 8.75)	0.00 (0.00, 0.00)	<0.001
SPT Birch Pollen (mm)	7.00 (4.00, 8.00)	0.00 (0.00, 0.00)	<0.001
SPT Timothy Grass (mm)	7.75 (4.00, 14.00)	0.00 (0.00, 0.00)	<0.001
Total IgE (kU/L)	529 (150, 1314)	21 (11, 54)	<0.001
sIgE (kU/L)	20 (8, 72)	NA	NA
Cor a 9 (kU/L)	1 (1, 10)	NA	NA
Cor a 14 (kU/L)	8 (2, 41)	NA	NA

Note: Demographics characteristics of the hazelnut cohort and nonallergic controls. Key clinical parameters include age, sex, comorbidities, skin prick test (SPT) results, and serum IgE total and specific (sIgE) levels (kU/L = kilo units per litre). NA indicates cases where no data is available.
[a]In the patient columns, the data is formatted either as the number and percentage of participants in each category or as Median (Q1, Q3).
[b]The p-value is calculated by Wilcoxon rank sum test or Pearson's Chi-squared test.

RNA/miRNA Universal kit, Zymo Clean & Concentrator-5 kit, and TRIzol-chloroform protocols. Cell culture supernatant containing secreted proteins was stored at −80°C. DNA concentration and purity were assessed using a Nanodrop. DNA was stored at −20°C. RNA integrity (RIN) of diluted RNA was quantified using the RNA 6000 p Bioanalyser kit. All RNA samples presented with a RIN ≥ 8 and were used for mRNA sequencing.

2.5 | Profiling and Analysis of DNA, RNA, and Protein Data

DNA samples were randomized and processed on the Infinium MethylationEPIC v1.0 array. Raw .idat files were processed using Minfi. Normalization was performed using single-sample normal-exponential out-of-band (ssNOOB) and Beta-MIxture Quantile dilation (BMIQ). Cell composition was estimated using DNA methylation data (Figure E1, Table E3). The following QC metrics were used: Probes with low detection and bead counts, as well as known problematic probes were excluded. Samples were excluded based on low detection quality, low bead count, and outlier data including sex mismatch. Two individuals were excluded for sex mismatch and 725,817 probes remained for statistical analysis after QC. Differentially methylated probes (DMPs) were identified using the limma Bioconductor package at a genome-wide significance threshold of 9E−08 [20, 21]. The Enmix comb-p algorithm was used to identify differentially methylated regions (DMRs) [22]. Significant DMRs were defined as regions represented by at least three probes and a Šidák-corrected $p \leq 0.05$. Annotatr was used to annotate DMRs using the hg38 genome as reference [23]. DNA methylation analyses were re-run after excluding age-associated CpGs to confirm that reported associations were not driven by age [24]. Additionally, due to potential confounding, the methylation data was re-analysed after excluding individuals of non-European ancestry to confirm all major reported signals remained and were not driven by population-specific variation. Methylation beta-values were converted into M-values for statistical analysis.

Total RNA was processed using the Truseq Stranded mRNA Library Prep Kit. The Spliced Transcripts Alignment to a Reference (STAR) aligner was used to map and count gene transcripts. Genes with lowly mapped reads across groups were excluded. Differential gene expression was performed using DESeq2 [25]. Differentially expressed genes (DEGs) were defined having a false discovery rate (FDR)-adjusted p-value of <0.05 ($p_{FDR} \leq 0.05$) as well as an absolute log2 fold change (log2FC) ≥ 0.3.

Thawed cell culture supernatants (40 μL) were randomized into 96-well plates and processed using the Olink Target 96 inflammation panel. After QC excluding lowly detected signals, 74 of 92 proteins were retained in the final analysis. Differentially expressed proteins (DEPs) were defined as $p_{FDR} \leq 0.05$.

As an additional analysis, the Multi-Omics Factor Analysis framework (MOFA2) was used to integrate DNA methylation, RNA expression, and inflammatory protein data in an unsupervised manner. A single joint model was trained across all samples after harmonizing data across omics layers and retaining the 5000 most variable DNA methylation, 5000 RNA, and 74 protein features. We identified latent factors capturing the principal sources of variation in this data set. Variance explained and feature weights were extracted to aid factor interpretation, and latent factors were subsequently tested for association with (i), hazelnut allergy status and (ii) the effect of hazelnut stimulation. To understand the biological role of the associated latent

factors, we performed functional enrichment analyses using the Enrichr platform in R [26–28].

For hypergeometric tests, the R function phyper was used. Here, the background/universe were set to the number of unique genes in the respective omics analysis after quality control.

In total, 218 nonallergic and 46 hazelnut-allergic samples were used in the final analysis. Analyses were performed in R version 4.3.2 (2023-10-31). RNA demultiplexing and mapping were used in the bash environment. Various covariates were adjusted for in the dataset including age, sex, batch, and methylation chip positions. Table E4 describes the statistical models used in this data and detailed methods can be found in Supporting Methods.

2.6 | eQTM and Gene Expression Protein Analysis

Methylation-gene expression Pearson correlation analysis was performed to capture expression quantitative trait methylation signatures (eQTMs). Methylation-DEG correlations with $p_{FDR} \leq 0.05$ were considered significant. EnhancerAtlas 2.0 was used to predict putative promoter and enhancer signatures of DMR coordinates [29]. For gene expression-protein Pearson correlations, DEGs and DEPs were overlapped. $p_{FDR} \leq 0.05$ signatures were considered significant. The psych R package was used to statistically compare correlation coefficients between allergic and nonallergic groups, allowing assessments of whether correlation slopes differed significantly between groups over multiple omics layers ($p_{r.test} \leq 0.05$) [30].

2.7 | Functional Enrichment

Enrichment was performed in R using the gprofiler2 package [31]. Significant terms were defined as $p_{FDR} \leq 0.05$, with a minimum query overlap of 4 and term size of 10. Input genes included DMP-/DMR-associated genes (methylation), DEGs (transcriptomics), and DEPs (proteomics). Gene Set Enrichment Analysis (GSEA) was performed using "fgsea" in R, with DEGs ranked by log2FC [32]. The human Molecular Signature Database (MSigDB) (v2023.2.Hs) gene sets (term size 15–500) were used; $p_{FDR} \leq 0.01$ was considered significant. Protein–protein interaction (PPI) networks were generated with STRING [33]. Clustering was performed with the STRING mcl algorithm using the default inflation parameter of three.

3 | Results

Study participants were 24 individuals with OFC-confirmed hazelnut allergy and 109 without hazelnut allergy or sensitization (see Supporting Methods). Baseline characteristics are shown in Table 1. As expected, allergic participants had higher rates of eczema, asthma, pollen and grass sensitization, and hazelnut-specific IgE, with no significant sex differences between groups. We detected no significant association between age and the maximum tolerated dose during OFC in this cohort (Spearman's rho 0.2, $p = 0.5$; Figure E1).

3.1 | Differentially Methylated Regions With Immune Relevance Detected in Hazelnut Allergy

DNA methylation was profiled in PBMCs from hazelnut-allergic and nonallergic individuals under quiescent and hazelnut-stimulated conditions. First, we examined individual cytosine-phosphate-guanine (CpG) sites to highlight differentially methylated probes (DMPs). As DNA methylation often spans clusters of neighboring CpGs, we additionally examined differentially methylated regions (DMRs) to detect broader and more biologically relevant methylation patterns.

Case–control analysis of quiescent samples identified a single hypomethylated DMP (cg07322512, logFC = −0.29; $p = 7.12E-08$; Table E5) in a CpG shore near *SIX3* (Figure 1a). In hazelnut-stimulated samples, a hypomethylated DMP overlapping the first exon of *MFHAS1* (cg03899721, logFC = −0.41; $p = 6.8E-08$) reached genome-wide significance. Additionally, we detected 38 DMRs in quiescent and 46 in stimulated samples (Figure E1, Table E6). Significant DMRs were detected in both analyses, showing modest but consistent methylation differences, with similar effect sizes in both conditions (Figure 1b). A significant overlap in DMR-associated genes was observed between quiescent and stimulated samples (29.1%; $p_{hyper} \leq 0.01$), with 22 (27.8%) and 34 (43.0%) genes unique to each condition, respectively (Figure 1c).

Overlapping genes included *GALNT5* (quiescent), as well as the immune-related *IL13/TH2LCRR*, *IL32*, and *MFHAS1* (shared; Figure 1c, Table E6). In quiescent samples, a hypermethylated DMR overlapped the *GALNT5* promoter and first exon (chr2:157257557-157257913; $p_{Šidák} = 7.72E-05$; $logFC_{\mu} = 0.20$).

A DMR spanning the *IL32* promoter to second exon was significantly hypomethylated in hazelnut-allergic versus nonallergic individuals in both quiescent (Figure 1c; chr16: 3065285-3065809; logFC = −0.25; $p_{Šidák} = 4.91E-08$) and stimulated (chr16:3065551-3065809; logFC = −0.22; $p_{Šidák} = 6.88E-05$) samples. We likewise observed hypomethylated DMRs overlapping the first exon of *MFHAS1* (quiescent: chr8: 8891026-8891565; logFC = −0.31; $p_{Šidák} = 5.13E-04$; stimulated: chr8:8891026-8891834; logFC = −0.33; $p_{Šidák} = 1.32E-07$) as well as DMRs overlapping the antisense RNA gene *ZNF341-AS1* (quiescent: chr20:33810217-33810459; logFC = −0.53; $p_{Šidák} = 2.03E-02$; hazelnut-stimulated: chr20:33810217-33810459; logFC = −0.64; $p_{Šidák} = 3.82E-05$).

Two of the largest and highly significant hypomethylated DMRs in the HLA class I region showed consistent effects in hazelnut-allergic individuals irrespective of stimulation status (chr6:31307774-31308436/chr6:31307490-31308436; logFC ≈ −0.58; $p_{Šidák} \leq 1.43E-10$; and chr6:30127359-30127643/chr6:30127210-30127719; logFC ≈ −0.23; $p_{Šidák} \leq 2.44E-10$; Table E6). The latter DMR (chr6:30127359-30127643/chr6:30127210-30127719) was identified between the protein-coding genes *TRIM31* and *TRIM40*. A third, smaller hypomethylated DMR overlapping *CDSN* was also detected in

a

DMP	Condition	logFC	P value	Category	Gene overlap	Gene position
cg07322512	Quiescent	-0.29	7.1e-08	Shore	None	Intergenic
cg03899721	Hazelnut	-0.41	6.8e-08	Island	*MFHAS1*	5'UTR

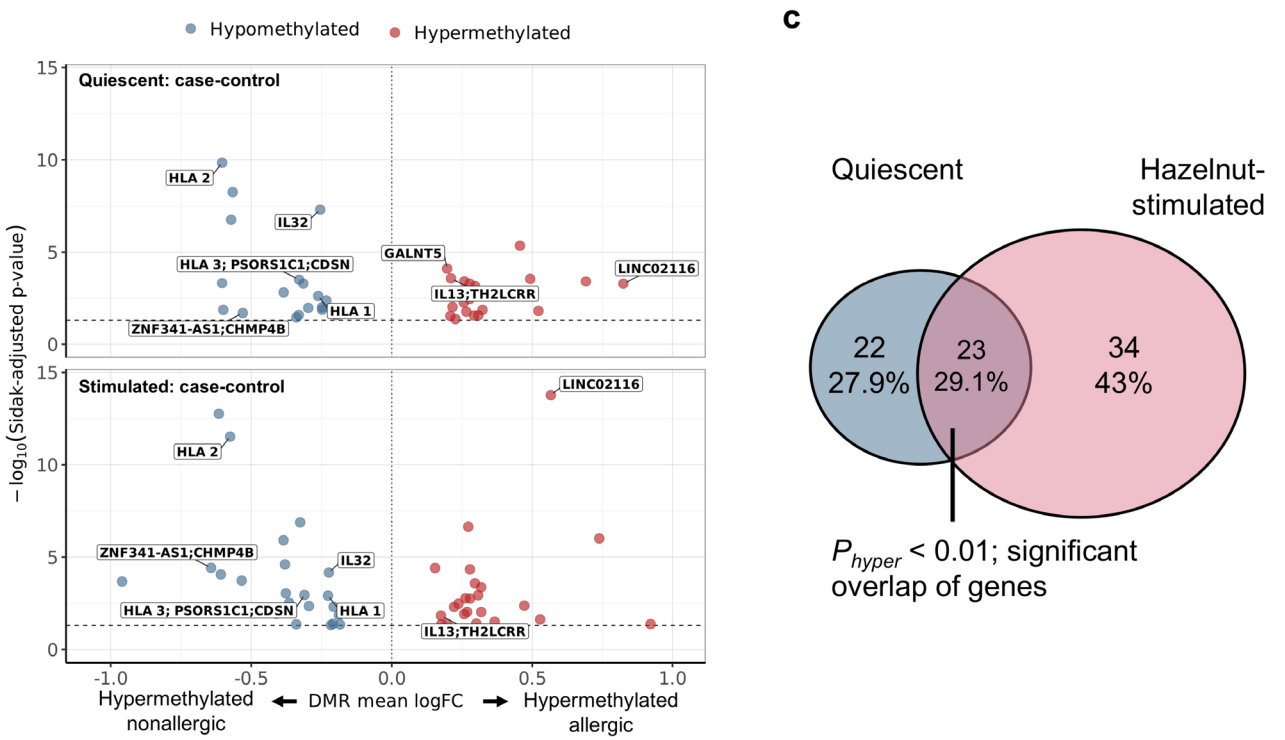


FIGURE 1 | DNA methylation case–control hazelnut overview. (a) Table showing the only two detected DMPs as well as information about these signals. DMP, differentially methylated probe; LogFC = log2 fold change; Category = CpG genomic context. (b) Volcano plot illustrating adjusted *p*-values and average effect sizes of each DMR, colored by quiescent (blue) and stimulated (red) analyses. Genes of interested are labelled. (c) Venn diagram depicting the DMR-associated genes and their overlap in quiescent and hazelnut-stimulated PBMCs.

both conditions (chr6:31120411-31120658; logFC ≈ −0.32; $p_{\text{Šidák}} \leq 1.12\text{E}{-}03$).

In contrast, a hypermethylated DMR was detected overlapping the first intron of *TH2LCRR* and upstream of *IL13* (chr5:132655799-132656076) in both conditions (quiescent: $\text{logFC}_{\mu} = 0.21$, $p_{\text{Šidák}} = 2.61\text{E}{-}04$; stimulated: $\text{logFC}_{\mu} = 0.17$, $p_{\text{Šidák}} = 1.48\text{E}{-}02$).

To assess group-condition responses to antigen, we performed an interaction analysis and identified one DMP (cg19017420) in a CpG shore upstream of *ARL2* on chromosome 11 ($p = 7.11\text{E}{-}08$, logFC = −0.47). No functional enrichment or transcription factor motif enrichment was observed for DNA methylation-associated genes in any methylation analysis.

All reported DMPs and DMRs remained statistically significant following the exclusion of known age-associated CpGs, suggesting these signals were not primarily driven by age (Supporting Methods; data not shown). Additionally, we studied genetic ancestry as a potential confounder. We reported three associations of individual DMPs (differentially methylated probes, cg07322512, cg03899721, cg19017420). At all three sites, no variant with minor allele frequency > 0.0002 was found in any reported ancestry based on whole genome sequences of 76,156 individuals in the Genome Aggregation Database [34]. Thus, genetic variation is unlikely to impact differential methylation at those three DMPs. Furthermore, following exclusion of all non-European study participants, all major reported DMRs replicated in this analysis (Table E7).

Gene expression analysis highlights Th2, activation machinery, and vitamin D-related genes. Gene expression of PBMCs revealed 14 differentially expressed genes (DEGs) in quiescent samples and 118 in stimulated samples, most of which were upregulated in allergic individuals (Figure 2a, Table E8). Seven DEGs (5.6%) overlapped analyses ($p_{\text{hyper}} \leq 0.05$; significant overlap of genes), while 88.8% were unique to the stimulated

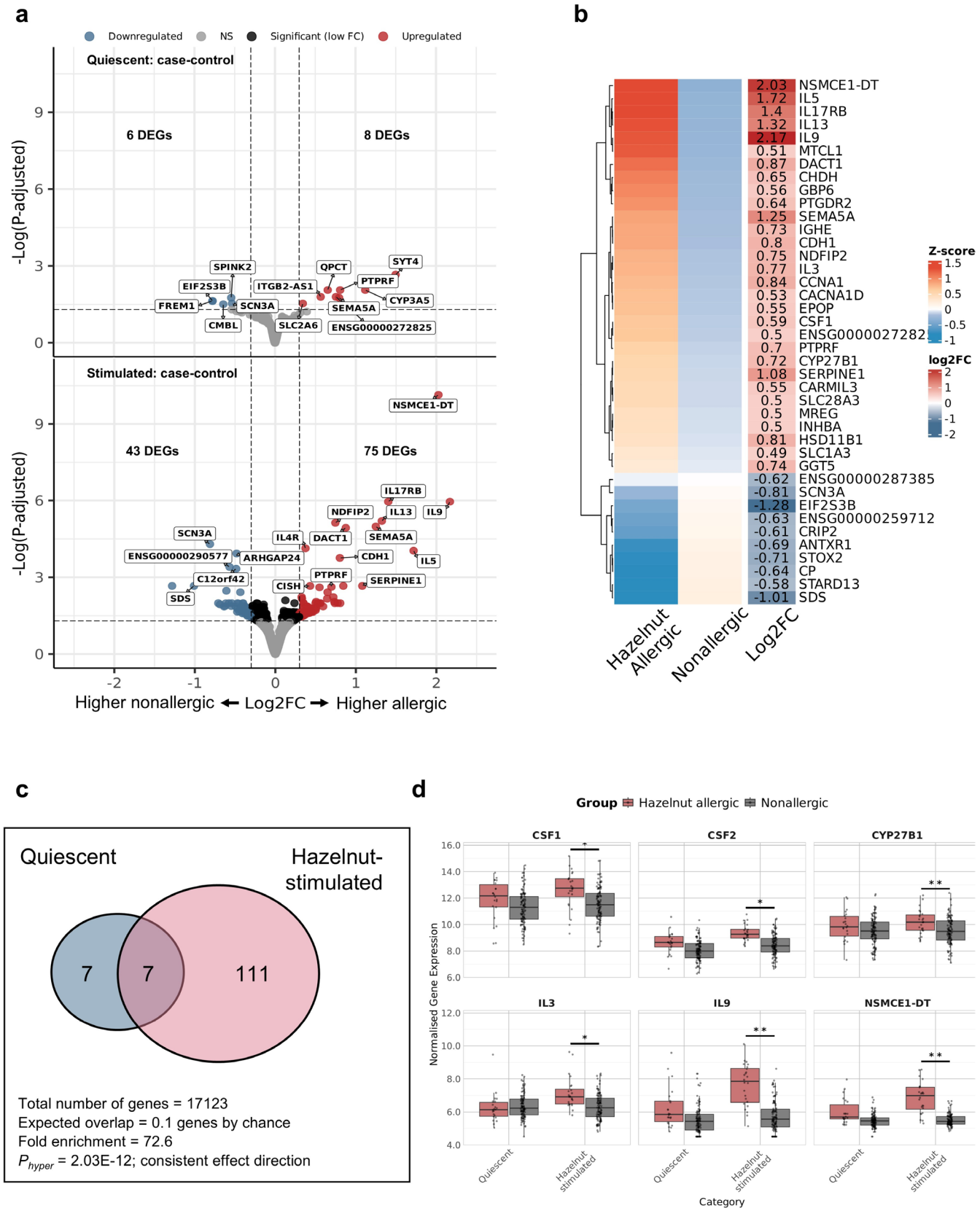


FIGURE 2 | Summary of case–control hazelnut DEGs. (a) Volcano plots depicting the DEGs in quiescent (top) and hazelnut-stimulated (bottom) case–control analysis. An absolute log2FC threshold of 0.3 was applied and highlighted beyond the vertical dotted line. The 20 most upregulated and 10 most downregulated genes are labelled, where possible. (b) Heatmap of average *Z*-scores for the top DEGs in the stimulated analysis. (c) Venn diagram showing the overlap of DEGs between analyses. (d) Boxplots illustrating a subset of the top immune- or allergy-related DEGs and their significance. Significant genes are marked by asterisks (*$p_{FDR} \leq 0.05$ and **$p_{FDR} \leq 0.01$). DEG, differentially expressed gene.

state (Figure 2c). Highly upregulated allergy-related genes included *IGHE*, *PTGDR2*, *IL9*, *IL17RB*, *IL13*, and *IL5* (Figure 2b). Additional stimulation-specific signals included *NSMCE1-DT*, *CSF1/2*, *IL3*, and *CYP27B1*. Top quiescent DEGs included *CYP3A5*, *SYT4*, *ITGB2-AS1*, *SEMA5A*, *FREM1*, and *HMOX1* (Figure E2).

To characterize biological processes linked to hazelnut allergy, we assessed enrichment of upregulated and downregulated genes using curated pathways. Key GO biological processes identified in hazelnut stimulated samples included cytokine responses, STAT signalling, immunoglobulin regulation, and cell growth (Figure 3a, Table E9). Upregulated genes in allergic individuals primarily drove these terms. KEGG analysis pinpointed JAK–STAT, FcεRI, and IL-17 signalling pathways, while Reactome enrichment pointed to interleukin signalling (Figure 3b). Using DEGs associated with hazelnut-allergy, we identified a core protein–protein interaction network of JAK–STAT and interleukin signalling (Figure 3c). JAK–STAT gene contributors included allergy-associated genes (*IL4R*, *IL5*, *IL9*, *IL13*), CSF genes (*IL3*, *CSF2*), as well as *CISH* and *IL2* (Figure E2). GSEA using the Hallmark gene sets highlighted E2F, MYC, G2M checkpoint, oxidative phosphorylation, TNF-α, STAT, and interferon response pathways in upregulated genes post-stimulation (Figure E2).

3.2 | JAK–STAT Signalling Enrichment in Differentially Secreted Proteins

We analysed differences in protein expression between allergic and nonallergic individuals as a highly functional readout of antigen stimulation. We observed similar numbers of DEPs in quiescent ($n=5$) and stimulated ($n=7$) samples (Figure 4a; Table E10). VEGFA and IL12β (IL-12/IL-23 subunit p40) were detected in both conditions. TNF (TNF-α) was elevated in allergic individuals under quiescent conditions, while TNF-β was increased post-stimulation (Figure 4a,c). KEGG analysis of stimulated samples identified three enriched pathways: "pathways in cancer", "JAK–STAT signalling" and "inflammatory bowel disease" (Table E11). PPI clustering confirmed modules related to JAK–STAT and inflammatory bowel pathways (Figure 4b), driven by IL-4, IL-13, IL-5, IL12β (IL-12/IL-23 subunit p40), and IFN-γ (Figure 4c). Interaction analysis of the protein data identified five DEPS with significant group-condition effects ($p_{FDR} \leq 0.05$; Figure E3). IL-2, IL-4, IL-5, IL-13, and TNF-β (*LTA*) were all more strongly induced in allergic individuals after antigen stimulation (log2FC = 0.83–1.07; $p_{FDR} \leq 0.04$).

3.3 | Multi-Omics Data Integration

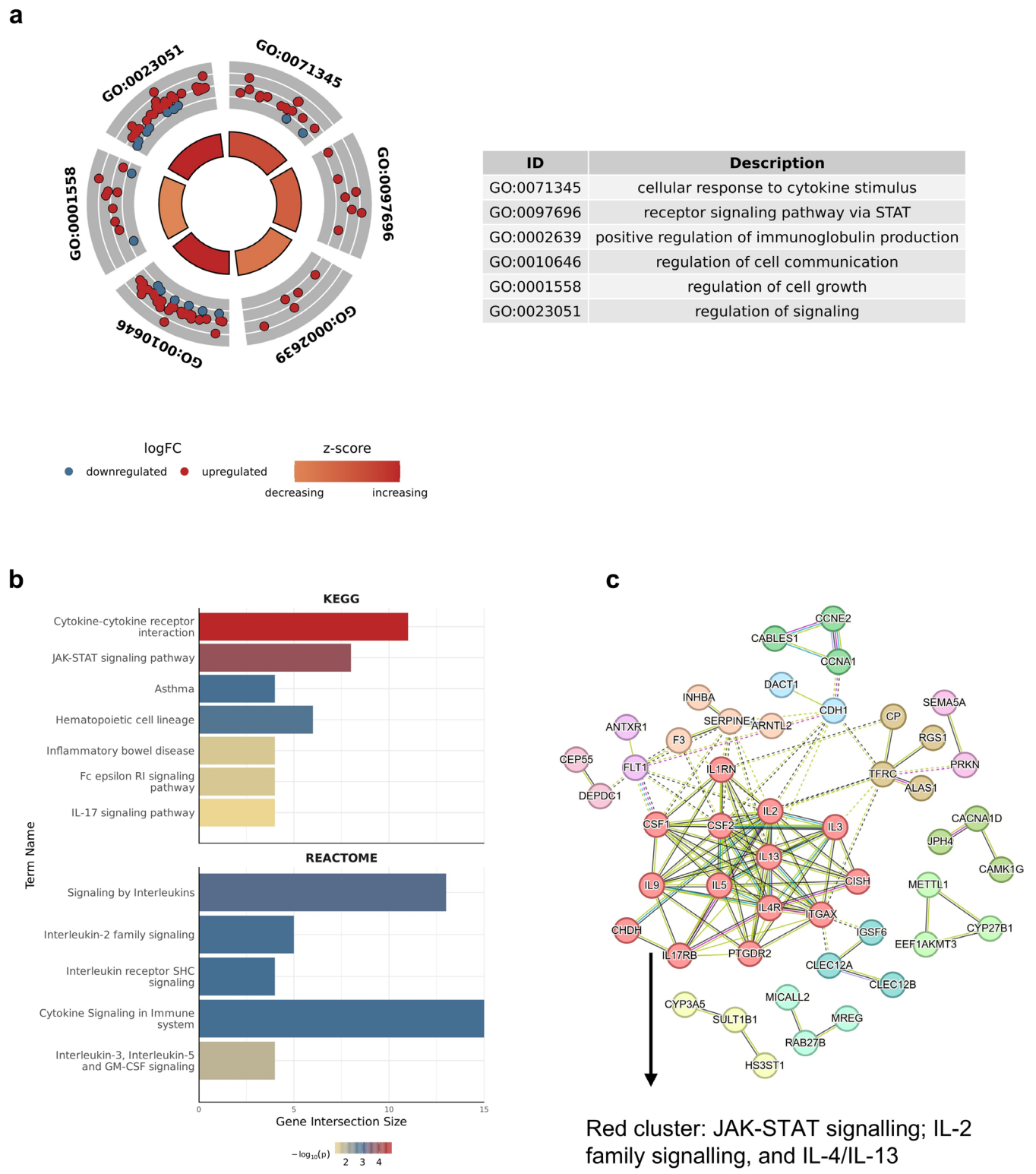
We integrated multi-omics data to characterize regulatory differences between hazelnut-allergic and nonallergic individuals under quiescent and antigen-specific conditions. eQTM analysis identified nine DEG-DMR pairs across five DMRs involving *IL5*, *IL13*, *CSF2*, and *IL3*, with *IL5* and *IL13* implicated in each analysis, although none of these correlations remained significant following multiple correction (Figure 5a; Table E12). Similarly, we tested for correlation of gene expression and protein secretion. Two strong DEG-DEP correlations were identified post-stimulation: *IL13* and *IL5* ($R>0.82$, $p_{FDR} \leq 0.001$; Figure 5b). Allergic individuals showed a strong correlation for both signals ($R>0.82$, $p_{FDR}<0.001$). In nonallergic individuals, *IL13* expression also showed a strong gene-protein correlation ($R=0.77$, $p_{FDR}=2.47E\text{-}22$), while *IL5* showed a much weaker correlation in these individuals, likely driven by a lack of gene expression ($R=0.31$, $p_{FDR}=0.001$). Importantly, correlating *IL5* ($p_{r.test}<0.001$), but not *IL13* ($p_{r.test}<0.57$), gene expression and protein levels could discriminate between allergic and nonallergic individuals.

Furthermore, we used the MOFA framework to integrate and analyse multi-omics data. We found that most variation in this study was contributed concordantly by gene expression and protein data, although the size of the protein input was much smaller. In contrast, only factor 4 showed a strong and distinct DNA methylation signal (Figure 6a). Most of the variance was concentrated in latent factors 1 and 2, both of which were significantly associated with the case–control status in quiescent or stimulated samples, respectively (Figure 6b). In addition, Factors 3 and 5 were associated with the response to hazelnut stimulation. Gene enrichment was performed within each of these factors across omics data. Factors 1, 2, 3 and 5 were dominated by immune-related terms. Factor 1 was characterized by enrichment of inflammatory response pathways, Toll-like receptor signalling, phagocytosis, efferocytosis, and responses to bacterial products and lipopolysaccharide supporting activated innate immune sensing and phagocyte-driven inflammation, while factor 2 was distinguished by a strong interferon- and chemokine-driven antiviral signature. Factor 3 showed wide overlap with factor 1; however, it showed a stronger IL-17/TNF signalling enrichment, while factor 5 was marked by bacterial/LPS responses driven by myeloid cells and neutrophils. While the methylation-specific factor 4 was also significantly associated with the case–control status, it only showed sparse enrichment primarily for nervous system development and cell adhesion pathways (Figure 6c).

4 | Discussion

Hazelnut allergy is a major cause of food-related anaphylaxis, yet remains poorly characterized molecularly [35]. We used antigen-specific multi-omics profiling to compare immune responses in hazelnut-allergic and nonallergic individuals and identify disease mechanisms and candidate molecular targets.

Epigenetic alterations mediate genetic and environmental effects in complex diseases [36, 37], including hazelnut allergy. We found a highly significant overlap between hazelnut allergy-associated DNA methylation patterns with and without antigen stimulation. This finding confirms the robustness of our technical workflow providing experimental replication of the methylation measurements. In stimulated cells, the top hypomethylated DMR overlapped the antisense transcript of *ZNF341*, *ZNF341-AS1*; in quiescent cells, this region remained similarly hypomethylated. Interestingly, homozygous nonsense mutations in *ZNF341*, which encodes a zinc finger transcription factor, have recently been shown to cause autosomal recessive hyper-IgE syndrome. ZNF341 binds to the *STAT3* promoter and is required for its transcriptional activation [38]. Notably, *STAT3* mutations cause autosomal dominant



ID	Description
GO:0071345	cellular response to cytokine stimulus
GO:0097696	receptor signaling pathway via STAT
GO:0002639	positive regulation of immunoglobulin production
GO:0010646	regulation of cell communication
GO:0001558	regulation of cell growth
GO:0023051	regulation of signaling

FIGURE 3 | Functional enrichment of genes associated with hazelnut allergy detected after hazelnut stimulation. (a) GOplot summarizing the top key driver terms associating with hazelnut allergy. Terms are ordered by their position on the plot axis. Genes contributing to the terms are shown as red (positive logFC/upregulated) or blue (negative logFC/downregulated). A *z*-score indicated the balance of up- versus downregulated genes contribute to each term. Darker red indicates, for example, that more upregulated genes contribute to the GO term. (b) All of the KEGG and Reactome terms associating with hazelnut allergy. (c) Protein–protein interaction network of DEGs highlighting a core cluster of genes involved in the JAK–STAT signalling and IL-signalling pathways. DEG, differentially expressed gene; GO, gene ontology; logFC, log2 fold change.

hyper-IgE syndrome impairing cytokine signalling, Th17 cell development, and epithelial repair [39], and often featuring food allergy [40]. We detected another hypomethylation signal implicating *STAT3* dysfunction, a DMP overlapping the *ARL2* promoter, a gene with diverse functions that is also required for nuclear retention of activated *STAT3* [41]. Our results

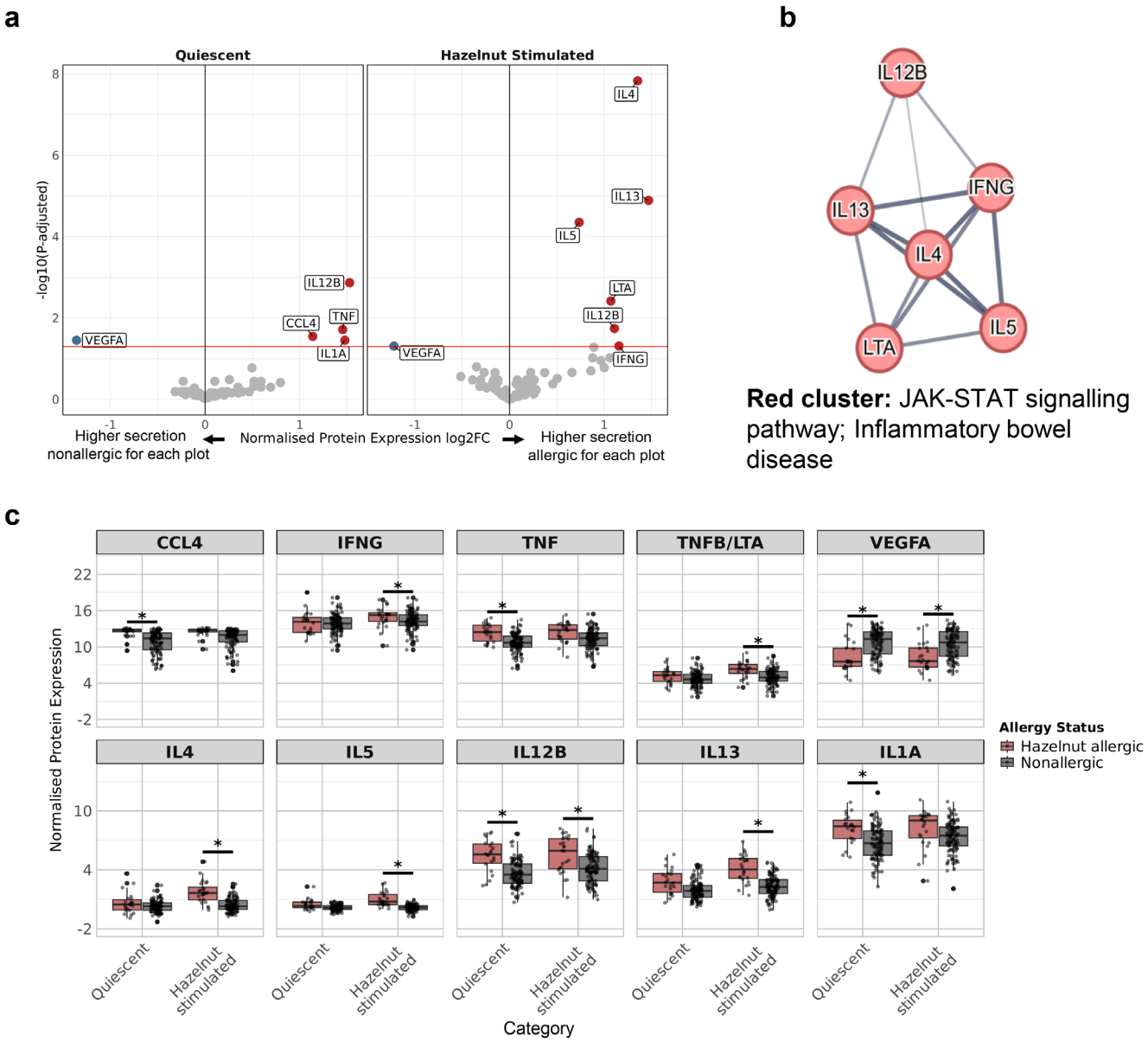


FIGURE 4 | Summary of DEPs detected in hazelnut case–control analysis from 48-h cell culture supernatant. (a) Volcano plots highlighting all the DEPs found in the case–control quiescent (left) and hazelnut-stimulated (right) analyses. (b) Protein–protein interaction DEPs from hazelnut-stimulated samples showing a cluster involved in JAK–STAT signalling. (c) Boxplots highlighting all DEPs. DEP, differentially expressed protein.

suggest epigenetic alterations at the *ZNF341* and *ARL2* locus to be involved in STAT3-mediated IgE dysregulation in hazelnut allergy [42].

We identified a hypermethylated DMR overlapping the first exon of the *long non-coding T Helper Type 2 Locus Control Region Associated RNA* (*TH2LCRR*) which is known to upregulate the expression of Th2 cytokines *IL4*, *IL5*, and *IL13* [43, 44]. The DMR is located 14 kb upstream of the dominant *TH2LCRR* isoform in immune cells (transcript ENST00000457489.1, exons 4–7, GTEx [45]). While hypermethylation is mostly associated with decreased gene expression, a recent genome-wide study in whole blood found that it is associated with increased expression in 34% of cases [46]. Our findings suggest that hypermethylation of this DMR may mediate the upregulation of IL-4, IL-5, and IL-13 cytokine expression, which we also detected.

Furthermore, integration of RNA and protein data revealed that *IL5*, but not *IL13*, showed a stronger group-separating signal between allergic and nonallergic individuals. Importantly, this result assesses differences in association patterns rather than diagnostic performance of these two markers, and no classification metrics (e.g., sensitivity or specificity) were derived. Further studies are required to evaluate its potential as disease-specific biomarker. Our data emphasize the importance of antigen-specific stimulation for its detection.

Enrichment of differentially expressed genes highlighted canonical pathways in hazelnut allergy: FcεRI signalling, type-2 cytokine signalling (IL-4, IL-5, IL-13), and the JAK–STAT pathway. These pathways are linked with FcεRI activation releasing Th2 cytokines which signal through the JAK–STAT pathway, thus bridging the immediate effector response to the longer-term

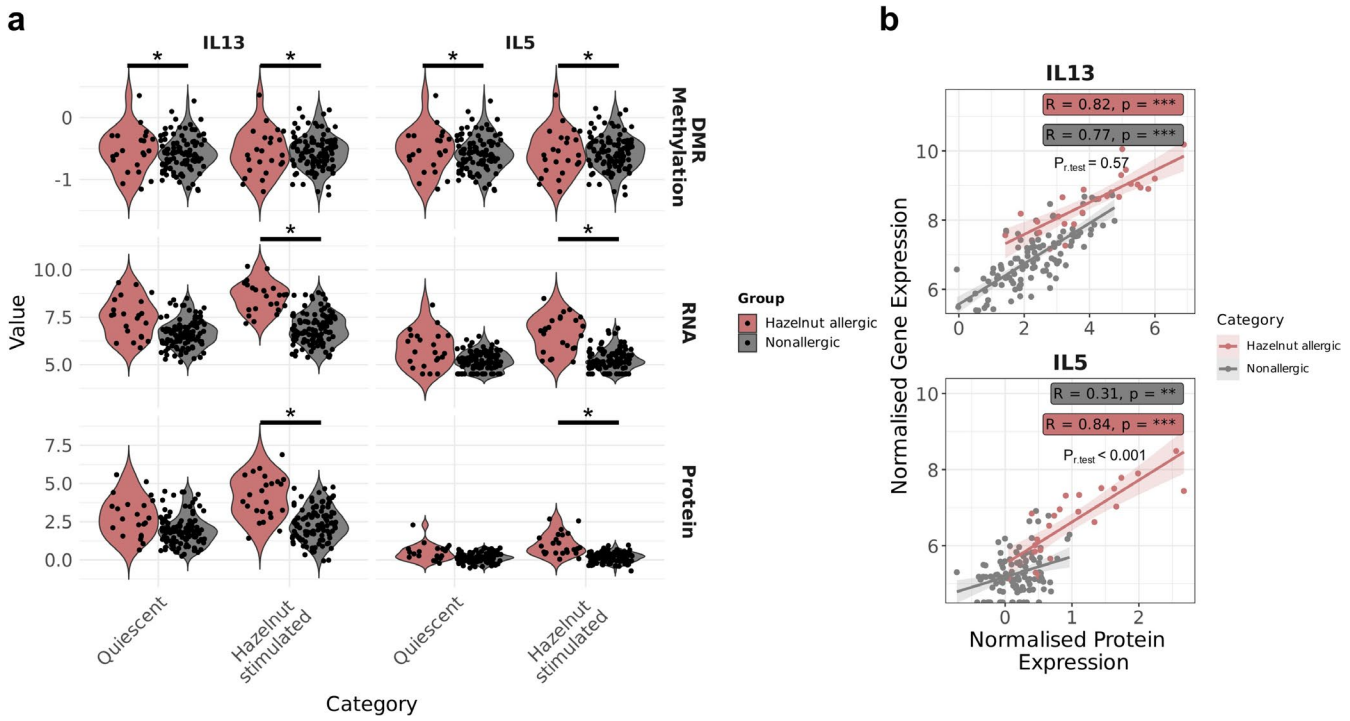


FIGURE 5 | Multi-omics analysis of *IL5* and *IL13* in hazelnut case–control samples. (a) Violin plots showing a single DMR (top) that potentially interacts with *IL5* and/or *IL13* in the gene expression (middle) and protein (bottom) data layers. Significance is denoted by asterisks ($p_{FDR} \leq 0.05$). (b) Pearson correlations of gene expression and protein expression data for *IL5* and *IL13*.

transcriptional programs that sustain and amplify disease. This underscores the IL-4/IL-13-JAK/STAT axis as a potential therapeutic target. Notably, JAK1/2 inhibitors are approved for atopic dermatitis and have shown promising results for asthma [47], with a phase I pilot trial testing the JAK1 inhibitor abrocitinib in food allergy (NCT05069831). In addition, latent factor analysis in the integrated multi-omics data identified four major immune-associated transcriptional programs (factors 1, 2, 3, and 5) that explained most of the molecular variation in the dataset. The dominant factors 1 and 2 were associated with the case–control status, each contributing up to 20% of variance for both mRNA and protein expression. Both factors appeared to represent complementary but distinct components of innate immunity with factor 1 reflecting upstream microbial sensing and phagocyte activation, whereas factor 2 reflected downstream interferon-associated inflammatory recruitment and antiviral responses. Thus, the main multi-omics variation distinguishing cases from controls in this data set implicated expression programs of antimicrobial, antiviral, and cytokine-mediated innate immune activation in hazelnut allergy. Notably, by investigating cord blood of newborns who later developed food allergy, Zhang et al. found a hyperresponsive innate immune state at birth, which, together with exposure to the mucosal cytokine TGF-b, suppressed IL-2 expression by CD4+ T cells promoting nonclassical TH2 differentiation [48]. Furthermore, Neeland et al. found an increased number of circulating myeloid dendritic cells and monocytes expressing higher levels of HLA-DR and elevated production of TNF-a, IL-6, IL-1b, and IL-8 upon in vitro endotoxin stimulation in 1 year old infants with hen's egg allergy [49]. Taken together, these studies demonstrated that an innate hyper-inflammatory phenotype at birth and in the first year of life are associated with food allergy. Our results suggest that dysregulated innate immune responses are also involved in hazelnut allergy beyond infancy in later childhood and adulthood. Further studies are required to elucidate the molecular mechanisms underlying the multi-omics differences observed.

The HLA region, central to antigen presentation, is frequently associated with food allergy. In hazelnut-allergic individuals, we identified three hypomethylated DMRs in the HLA class I region, all present with and without hazelnut stimulation and displaying similar effect sizes within conditions. The first lies between *TRIM31* and *TRIM40*, ubiquitin ligases involved in antiviral immunity and excessive inflammation response [50]. Interestingly, upregulated intestinal *TRIM40* expression has been found in chronic inflammatory bowel disease and intestinal epithelial barrier deficiency which may also play a role in hazelnut allergy [51]. The second overlaps corneodesmosin (*CDSN*), where homozygous loss has been associated with severe skin barrier deficiency and food allergy [52]. Thus, our study identifies epithelial barrier genes of the gut and skin, extending previous findings on the genetic risk for hazelnut allergy conferred by loss-of-function mutations in the skin barrier gene filaggrin [53]. The third lies between HLA-B and HLA-C, genes not previously linked to food allergy, and is the closest DMR (~1.7 Mbp) to a known hazelnut-associated genetic locus [13].

CYP27B1 (*25-hydroxyvitamin D3 1-alpha-hydroxylase*), which converts calcidiol [25(OH)D3] to biologically active vitamin D (calcitriol, 1,25(OH)2D3), was upregulated upon stimulation in allergic individuals [54]. Interestingly, the role of vitamin D is further supported by the hypomethylation of a DMR spanning promotor and first exon of *IL32*. IL-32 upregulates CYP27B1 and vitamin D receptor (VDR) expression [55]. The

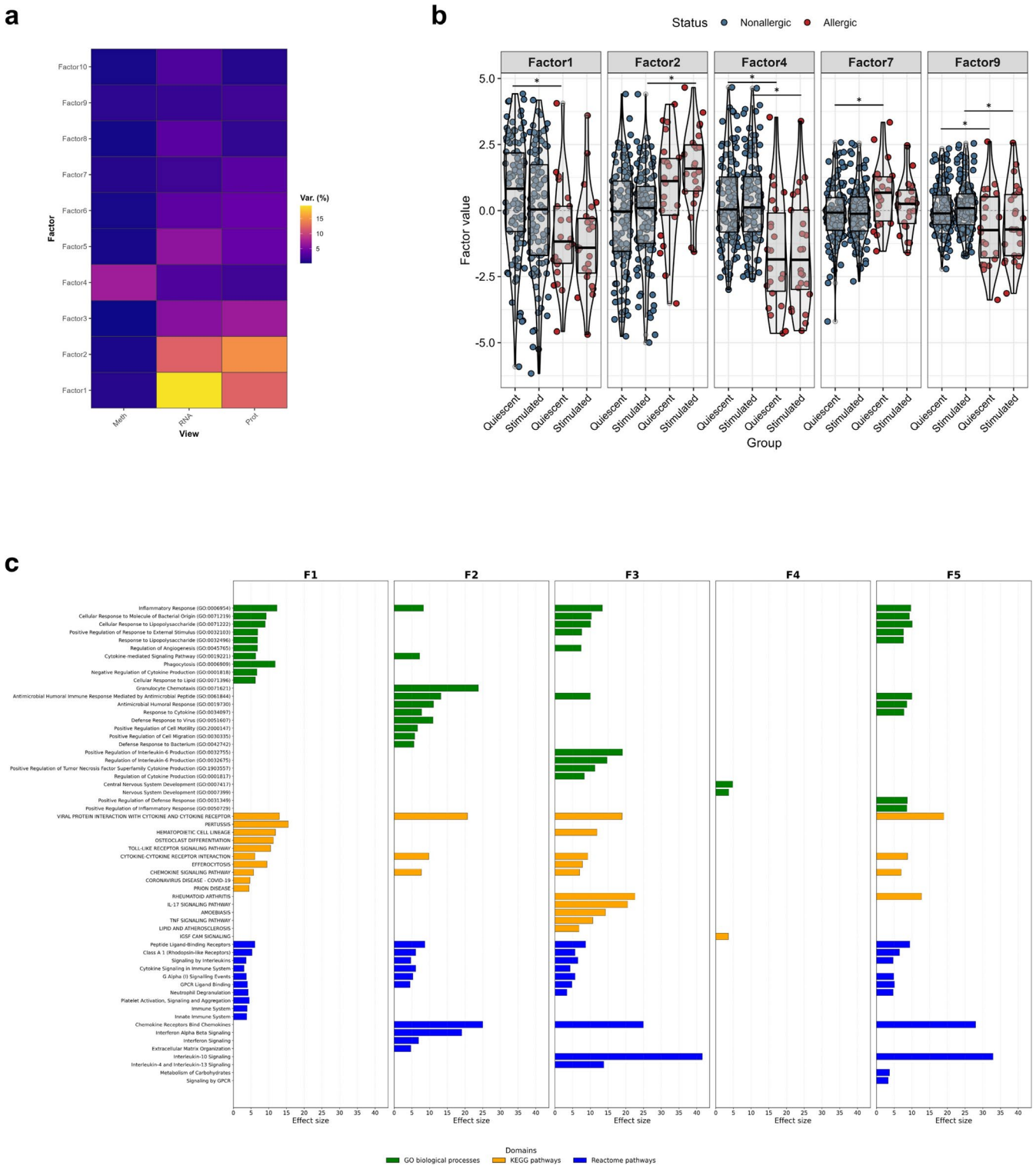


FIGURE 6 | Multi-omics factor analysis of hazelnut data. (a) Variance decomposition showing contribution of each omics layer to the variability in data, stratified by latent factor. (b) Violin plots depicting latent factors associated with hazelnut allergy. (c) Enrichment plots across five latent factors (F1–F5), showing the top 10 (where applicable) associated gene sets ($p_{\text{FDR}} \leq 0.05$ and $10 \geq$ overlapping query genes) for the gene ontology biological processes (green), KEGG pathways (orange), and reactome pathways (blue). Bar length indicates the odds ratio/effect size. Terms are shown only when they rank within the top 10 for the corresponding factor and database; effects for terms outside this range are omitted.

complex role of vitamin D in allergic disease has been widely investigated, with both deficiency [56] and excess [57–59] of vitamin D exposure associated with an increased risk of allergy. Interestingly, a randomized, controlled trial of daily vitamin D supplementation in the first year of life found that higher vitamin D levels in cord blood were associated with higher risk of food allergen sensitization. Moreover, high-dose vitamin D supplementation was associated with an increased risk of milk

allergy [60]. Vitamin D has also previously been shown to be related to elevated IgE concentrations, although we could not confirm whether this relationship is replicated in our dataset [61]. Interestingly, autocrine vitamin D signalling has been shown to regulate inflammatory networks, which may suggest its role in anti-inflammatory responses during cell activation, potentially reflecting an attempted regulatory response to allergen stimulation [62]. Our findings also indicate an upregulation of the vitamin D pathway in hazelnut allergy, although targeted studies examining the pro-inflammatory nature of this response are warranted. To our knowledge, this is the first molecular evidence implicating vitamin D in hazelnut allergy.

Additional methylation and expression signals point to new hazelnut allergy biology. DMRs at *PHACTR1*, *MFHAS1*, and *SPRED2* replicate findings from peanut-allergy studies [63, 64], even though their role in food allergy remains unknown. In quiescent cells, the promoter/first exon of *GALNT5*, an O-glycosylation enzyme, was hypomethylated. Along with previous EWAS associations of *GALNTL4* [64, 65], our findings extend interest in the GalNAc-T gene family in food allergy. However, since this signal did not replicate following removal of non-European individuals, it should be interpreted with caution. Transcriptomically, the most induced transcript after stimulation in allergic individuals was the lncRNA *NSMCE1-DT*; variants at *NSMCE1* associate with eczema and asthma [66, 67]. Although these gene functions remain undefined, they highlight plausible contributors to hazelnut allergic responses and identify candidates for further investigation.

We also note that, at a protein level, allergic samples secreted more TNF (TNF-α) in quiescent cultures and higher LTA (TNF-β) after stimulation, suggesting both constitutive and inducible activation of the TNF-superfamily inflammatory signalling under different conditions [68]. Increased IL12β (IL-12/IL-23 subunit p40) was likewise compatible with activation of antigen-presenting-cell cytokine networks, as IL12β encodes the p40 subunit shared by IL-12 and IL-23 which are classically produced by activated myeloid cells that signal through JAK–STAT pathways [69–71]. By contrast, VEGFA (VEGF-A) was lower in allergic individuals, regardless of condition. In this ex vivo setting, this may reflect altered immune-vascular crosstalk or reduced leukocyte-derived angiogenic signalling. As VEGF-A regulation is highly context dependent and VEGF-A is frequently linked to vascular remodelling in allergic disease [72, 73], this observation warrants further investigation.

Although prior studies reported associations with hazelnut allergy, we did not observe overlapping signals in our dataset. This likely reflects differences in cohort definitions (OFC-confirmed hazelnut allergy vs. heterogenous or non-OFC cohorts), study design (antigen-specific stimulation at 48-h vs. baseline comparisons), and data type (multi-omics epigenetics, transcriptome, and protein data vs. genetic or transcriptomic alone). No previous work has examined hazelnut allergy using DNA methylation or multi-omics approaches. Strengths of this study include a well-phenotyped study cohort, strict phenotype definition, the use of antigen-specific stimulation, and stringent QC pipelines. The absence of genomic inflation, concordant signals across conditions, and recovery of known allergy genes and proteins support the data robustness. This data demonstrated that antigen stimulation was required to reveal meaningful hazelnut-specific transcriptional and proteomic signals, but the same was not true for DNA methylation, aligning with long-term stable epigenetic remodelling. Limitations include the use of PBMCs (limiting cell-specific resolution), the age imbalance, and a single 48-h timepoint which will have missed dynamic regulatory changes. A small sample size likely resulted in a limited detection of group-specific effects and interactions. Since age-matched controls were not available, we mitigated age effects by both incorporating age as a covariate in the statistical models. We also noted that age was not significantly correlated with the maximum tolerated dose during OFC in this cohort. Moreover, we demonstrate that the reported differences in DNA methylation were not due to known age-associated probes. While our sample size did not allow for an independent replication, future studies with larger cohorts will be essential to confirm and extend these findings.

In summary, this study provides a detailed overview of differentially expressed and methylated genes and proteins associated with hazelnut allergy. In addition to confirming established pathways such as type-2 cytokine, FcεRI and the JAK–STAT signalling, we identified several findings that extend the current literature. These include disease-associated signals that were detected only after hazelnut-specific stimulation, overlap with genes implicated in monogenic hyper-IgE disorders at a methylation level which was surprising given the monogenic nature of this syndrome, association to the vitamin D pathway at both a transcriptomics and methylation level, and involvement of intestinal and cutaneous epithelial barrier genes at a methylation level. Overall, we provide a multi-omics signature of hazelnut allergy, representing the largest known cohort of hazelnut-allergic and nonallergic individuals investigated using antigen-specific multi-omics profiling. These findings provide a catalogue of candidate biomarkers to guide future mechanistic studies and prospective validation.

Author Contributions

Conceptualization: I.M., K.B., M.W., Y.-A.L. Data Curation: A.C.S.N.J., A.A.-S. Formal Analysis: A.C.S.N.J. Funding Acquisition: I.M., Y.-A.L. Investigation: A.C.S.N.J., A.G., P.M., M.Z. Methodology: A.C.S.N.J., A.G., A.A.-S., I.M., Y.-A.L. Project Administration: A.C.S.N.J., I.M., K.B., M.W., Y.-A.L. Supervision: A.A.-S., I.M., Y.-A.L. Visualization: A.C.S.N.J. Writing – Original Draft Preparation: A.C.S.N.J., A.A.-S., I.M., Y.-A.L. Writing – Review and Editing: all authors.

Acknowledgments

We thank the Genomics facility at the Max Delbrück Center Berlin for sequencing the RNA samples. We are grateful to Susanne Blachut and Claudia Langnick for their support on RNA library preparation. We thank the Deutsche Forschungsgemeinschaft (DFG, German Research Foundation) for funding the clinical research unit (CRU339); Food allergy and tolerance (FOOD@)—409525714. Open Access funding enabled and organized by Projekt DEAL.

Funding

This work was funded by the Deutsche Forschungsgemeinschaft (DFG, German Research Foundation) as part of the clinical research unit (CRU339); Food allergy and tolerance (FOOD@)—(Grant 409525714), Aleix Arnau-Soler was supported by the Federal Ministry of Research,

Technology and Space: German Center for Child and Adolescent Health (DZKJ) (Grant 01GL2401B).

Conflicts of Interest

Kirsten Beyer reports advisory board/consulting fees or speakers bureau from Aimmune, Akademie Fresenius, ALK, Danone/Nutricia/Milupa, HAL, Infectopharm, Kantar Health, Primus Consulting, Viatris/Meda Pharma/Mylan/Mice, Nestle, Novartis, Stallergens and ThermoFisher as well as research grants from Aimmune, ALK, Danone/Nutricia/Milupa, DBV Technologies, Hipp, Hycor, Infectopharm, Nestle and Novartis outside the submitted work. Remaining authors have no conflicts to disclose.

Data Availability Statement

The data that support the findings of this study are available from the corresponding author upon reasonable request.

References

1. W. Loh and M. L. K. Tang, "The Epidemiology of Food Allergy in the Global Context," *International Journal of Environmental Research and Public Health* 15 (2018): 2043, https://doi.org/10.3390/ijerph15092043.

2. E. Hossny, M. Ebisawa, Y. El-Gamal, et al., "Challenges of Managing Food Allergy in the Developing World," *World Allergy Organization Journal* 12 (2019): 100089, https://doi.org/10.1016/j.waojou.2019.100089.

3. A. T. Clark, K. Anagnostou, and P. W. Ewan, "Cashew Nut Causes More Severe Reactions Than Peanut: Case-Matched Comparison in 141 Children," *Allergy* 62 (2007): 913–916, https://doi.org/10.1111/j.1398-9995.2007.01447.x.

4. V. McWilliam, J. Koplin, C. Lodge, M. Tang, S. Dharmage, and K. Allen, "The Prevalence of Tree Nut Allergy: A Systematic Review," *Current Allergy and Asthma Reports* 15 (2015): 54, https://doi.org/10.1007/s11882-015-0555-8.

5. G. C. I. Spolidoro, D. Lisik, S. Nyassi, et al., "Prevalence of Tree Nut Allergy in Europe: A Systematic Review and Meta-Analysis," *Allergy* 79 (2024): 302–323, https://doi.org/10.1111/all.15905.

6. J. Johnson, A. Malinovschi, K. Alving, J. Lidholm, M. P. Borres, and L. Nordvall, "Ten-Year Review Reveals Changing Trends and Severity of Allergic Reactions to Nuts and Other Foods," *Acta Paediatrica* 103 (2014): 862–867, https://doi.org/10.1111/apa.12687.

7. L. B. Grabenhenrich, S. Dölle, A. Moneret-Vautrin, et al., "Anaphylaxis in Children and Adolescents: The European Anaphylaxis Registry," *Journal of Allergy and Clinical Immunology* 137 (2016): 1128–1137.e1, https://doi.org/10.1016/j.jaci.2015.11.015.

8. M. Worm, K. Scherer, A. Köhli-Wiesner, et al., "Food-Induced Anaphylaxis and Cofactors - Data From the Anaphylaxis Registry," *Allergology Select* 1 (2017): 21–27, https://doi.org/10.5414/ALX01401E.

9. A. Giannetti, A. Ruggi, G. Ricci, G. Giannì, and C. Caffarelli, "Natural History of Hazelnut Allergy and Current Approach to Its Diagnosis and Treatment," *Children* 10 (2023): 585, https://doi.org/10.3390/children10030585.

10. M. Worm, A. Alexiou, V. Höfer, et al., "An Interdisciplinary Approach to Characterize Peanut-Allergic Patients-First Data From the FOOD@ Consortium," *Clinical and Translational Allergy* 12 (2022): e12197, https://doi.org/10.1002/clt2.12197.

11. A. Devonshire, Y. Gautam, E. Johansson, and T. B. Mersha, "Multi-Omics Profiling Approach in Food Allergy," *World Allergy Organization Journal* 16 (2023): 100777, https://doi.org/10.1016/j.waojou.2023.100777.

12. A. Arnau-Soler, S. E. Ashley, A. Ghauri, et al., "Understanding the Variability of Peanut-Oral Immunotherapy Responses by Multi-Omics Profiling of Immune Cells," *Allergy* 80 (2025): 3342–3358, https://doi.org/10.1111/all.16627.

13. Y. Sun, J. M. Vonk, E. T. G. Kersten, C. Qi, A. B. Sprikkelman, and G. H. Koppelman, "Genome-Wide Association Study Reveals a Causal Relationship Between Allergic Rhinitis and Hazelnut Allergy," *Allergy* 80 (2025): 309–318, https://doi.org/10.1111/all.16411.

14. S. Hand, C. Darke, J. Thompson, et al., "Human Leucocyte Antigen Polymorphisms in Nut-Allergic Patients in South Wales," *Clinical and Experimental Allergy* 34 (2004): 720–724, https://doi.org/10.1111/j.1365-2222.2004.1932.x.

15. M. M. Amoli, S. Hand, A. H. Hajeer, et al., "Polymorphism in the STAT6 Gene Encodes Risk for Nut Allergy," *Genes and Immunity* 3 (2002): 220–224, https://doi.org/10.1038/sj.gene.6363872.

16. W. H. Boehncke, C. Loeliger, P. Kuehnl, H. Kalbacher, B. O. Böhm, and H. Gall, "Identification of HLA-DR and -DQ Alleles Conferring Susceptibility to Pollen Allergy and Pollen Associated Food Allergy," *Clinical and Experimental Allergy* 28 (1998): 434–441, https://doi.org/10.1046/j.1365-2222.1998.00246.x.

17. K. H. Lee, A. Bosco, M. O'Sullivan, et al., "Identifying Gene Network Patterns and Associated Cellular Immune Responses in Children With or Without Nut Allergy," *World Allergy Organization Journal* 15 (2022): 100631, https://doi.org/10.1016/j.waojou.2022.100631.

18. V. Trendelenburg, S. Dölle-Bierke, N. Unterleider, et al., "Tolerance Induction Through Non-Avoidance to Prevent Persistent Food Allergy (TINA) in Children and Adults With Peanut or Tree Nut Allergy: Rationale, Study Design and Methods of a Randomized Controlled Trial and Observational Cohort Study," *Trials* 23 (2022): 236, https://doi.org/10.1186/s13063-022-06149-4.

19. FDA, *Guidance for Industry: Pyrogen and Endotoxins Testing: Questions and Answers* (FDA, 2024), accessed February 13, 2025, https://www.fda.gov/regulatory-information/search-fda-guidance-documents/guidance-industry-pyrogen-and-endotoxins-testing-questions-and-answers.

20. M. E. Ritchie, B. Phipson, D. Wu, et al., "Limma Powers Differential Expression Analyses for RNA-Sequencing and Microarray Studies," *Nucleic Acids Research* 43 (2015): e47, https://doi.org/10.1093/nar/gkv007.

21. G. Mansell, T. J. Gorrie-Stone, Y. Bao, et al., "Guidance for DNA Methylation Studies: Statistical Insights From the Illumina EPIC Array," *BMC Genomics* 20 (2019): 366, https://doi.org/10.1186/s12864-019-5761-7.

22. Z. Xu, L. Niu, and J. A. Taylor, "The ENmix DNA Methylation Analysis Pipeline for Illumina BeadChip and Comparisons With Seven Other Preprocessing Pipelines," *Clinical Epigenetics* 13 (2021): 216, https://doi.org/10.1186/s13148-021-01207-1.

23. R. G. Cavalcante and M. A. Sartor, "Annotatr: Genomic Regions in Context," *Bioinformatics* 33 (2017): 2381–2383, https://doi.org/10.1093/bioinformatics/btx183.

24. S. Horvath, "DNA Methylation Age of Human Tissues and Cell Types," *Genome Biology* 14 (2013): 3156, https://doi.org/10.1186/gb-2013-14-10-r115.

25. M. I. Love, W. Huber, and S. Anders, "Moderated Estimation of Fold Change and Dispersion for RNA-Seq Data With DESeq2," *Genome Biology* 15 (2014): 550, https://doi.org/10.1186/s13059-014-0550-8.

26. M. V. Kuleshov, M. R. Jones, A. D. Rouillard, et al., "Enrichr: A Comprehensive Gene Set Enrichment Analysis Web Server 2016 Update," *Nucleic Acids Research* 44 (2016): W90–W97, https://doi.org/10.1093/nar/gkw377.

27. E. Y. Chen, C. M. Tan, Y. Kou, et al., "Enrichr: Interactive and Collaborative HTML5 Gene List Enrichment Analysis Tool,"

BMC Bioinformatics 14 (2013): 128, https://doi.org/10.1186/1471-2105-14-128.

28. Z. Xie, A. Bailey, M. V. Kuleshov, et al., "Gene Set Knowledge Discovery With Enrichr," *Current Protocols* 1 (2021): e90, https://doi.org/10.1002/cpz1.90.

29. T. Gao and J. Qian, "EnhancerAtlas 2.0: An Updated Resource With Enhancer Annotation in 586 Tissue/Cell Types Across Nine Species," *Nucleic Acids Research* 48 (2020): D58–D64, https://doi.org/10.1093/nar/gkz980.

30. W. Revelle, *psych: Procedures for Psychological, Psychometric, and Personality Research* (2024), accessed February 13, 2025, https://cran.r-project.org/web/packages/psych/index.html.

31. L. Kolberg, U. Raudvere, I. Kuzmin, J. Vilo, and H. Peterson, "gprofiler2—An R Package for Gene List Functional Enrichment Analysis and Namespace Conversion Toolset g:Profiler," *F1000Research* 9 (2020): ELIXIR-709, https://doi.org/10.12688/f1000research.24956.2.

32. G. Korotkevich, V. Sukhov, N. Budin, B. Shpak, M. N. Artyomov, and A. Sergushichev, *Fast Gene Set Enrichment Analysis* (, 2021), https://doi.org/10.1101/060012.

33. D. Szklarczyk, R. Kirsch, M. Koutrouli, et al., "The STRING Database in 2023: Protein-Protein Association Networks and Functional Enrichment Analyses for Any Sequenced Genome of Interest," *Nucleic Acids Research* 51 (2023): D638–D646, https://doi.org/10.1093/nar/gkac1000.

34. S. Chen, L. C. Francioli, J. K. Goodrich, et al., "A Genomic Mutational Constraint Map Using Variation in 76,156 Human Genomes," *Nature* 625 (2024): 92–100, https://doi.org/10.1038/s41586-023-06045-0.

35. S. Dölle-Bierke, V. Höfer, W. Francuzik, et al., "Food-Induced Anaphylaxis: Data From the European Anaphylaxis Registry," *Journal of Allergy and Clinical Immunology: In Practice* 11 (2023): 2069–2079.e7, https://doi.org/10.1016/j.jaip.2023.03.026.

36. A. Arnau-Soler, B. L. Tremblay, Y. Sun, et al., "Food Allergy Genetics and Epigenetics: A Review of Genome-Wide Association Studies," *Allergy* 80 (2025): 106–131, https://doi.org/10.1111/all.16429.

37. S. M. Ho, A. Johnson, P. Tarapore, V. Janakiram, X. Zhang, and Y. K. Leung, "Environmental Epigenetics and Its Implication on Disease Risk and Health Outcomes," *ILAR Journal* 53 (2012): 289–305, https://doi.org/10.1093/ilar.53.3-4.289.

38. V. Béziat, J. Li, J. X. Lin, et al., "A Recessive Form of Hyper-IgE Syndrome by Disruption of ZNF341-Dependent STAT3 Transcription and Activity," *Science Immunology* 3 (2018): eaat4956, https://doi.org/10.1126/sciimmunol.aat4956.

39. Y. Minegishi, M. Saito, S. Tsuchiya, et al., "Dominant-Negative Mutations in the DNA-Binding Domain of STAT3 Cause Hyper-IgE Syndrome," *Nature* 448 (2007): 1058–1062, https://doi.org/10.1038/nature06096.

40. T. Al-Shaikhly and H. D. Ochs, "Hyper IgE Syndromes: Clinical and Molecular Characteristics," *Immunology and Cell Biology* 97 (2019): 368–379, https://doi.org/10.1111/imcb.12209.

41. R. Muromoto, Y. Sekine, S. Imoto, et al., "BART Is Essential for Nuclear Retention of STAT3," *International Immunology* 20 (2008): 395–403, https://doi.org/10.1093/intimm/dxm154.

42. S. Frey-Jakobs, J. M. Hartberger, M. Fliegauf, et al., "ZNF341 Controls STAT3 Expression and Thereby Immunocompetence," *Science Immunology* 3 (2018): eaat4941, https://doi.org/10.1126/sciimmunol.aat4941.

43. C. F. Spurlock, J. T. Tossberg, Y. Guo, S. P. Collier, P. S. Crooke, and T. M. Aune, "Expression and Functions of Long Noncoding RNAs During Human T Helper Cell Differentiation," *Nature Communications* 6 (2015): 6932, https://doi.org/10.1038/ncomms7932.

44. C. F. Spurlock, P. S. Crooke, and T. M. Aune, "Biogenesis and Transcriptional Regulation of Long Non-Coding RNAs in the Human Immune System," *Journal of Immunology* 197 (2016): 4509–4517, https://doi.org/10.4049/jimmunol.1600970.

45. J. Lonsdale, J. Thomas, M. Salvatore, et al., "The Genotype-Tissue Expression (GTEx) Project," *Nature Genetics* 45 (2013): 580–585, https://doi.org/10.1038/ng.2653.

46. A. Keshawarz, H. Bui, R. Joehanes, et al., "Expression Quantitative Trait Methylation Analysis Elucidates Gene Regulatory Effects of DNA Methylation: The Framingham Heart Study," *Scientific Reports* 13 (2023): 12952, https://doi.org/10.1038/s41598-023-39936-3.

47. H. Brooks W and Y. Renaudineau, "Not Just Another Klass (JAK) of Inhibitors for Allergies," *Journal of Allergy and Hypersensitivity Diseases* 1 (2024): 100001, https://doi.org/10.1016/j.jahd.2024.100001.

48. Y. Zhang, F. Collier, G. Naselli, et al., "Cord Blood Monocyte-Derived Inflammatory Cytokines Suppress IL-2 and Induce Nonclassic 'T(H)2-Type' Immunity Associated With Development of Food Allergy," *Science Translational Medicine* 8 (2016): 321ra8, https://doi.org/10.1126/scitranslmed.aad4322.

49. M. R. Neeland, J. J. Koplin, T. D. Dang, et al., "Early Life Innate Immune Signatures of Persistent Food Allergy," *Journal of Allergy and Clinical Immunology* 142 (2018): 857–864.e3, https://doi.org/10.1016/j.jaci.2017.10.024.

50. E. Chabot, D. Durantel, and J. Lucifora, "TRIM Proteins: A 'Swiss Army Knife' of Antiviral Immunity," *PLoS Pathogens* 21 (2025): e1013147, https://doi.org/10.1371/journal.ppat.1013147.

51. S. Kang, J. Kim, A. Park, et al., "TRIM40 Is a Pathogenic Driver of Inflammatory Bowel Disease Subverting Intestinal Barrier Integrity," *Nature Communications* 14 (2023): 700, https://doi.org/10.1038/s41467-023-36424-0.

52. V. Oji, K. M. Eckl, K. Aufenvenne, et al., "Loss of Corneodesmosin Leads to Severe Skin Barrier Defect, Pruritus, and Atopy: Unraveling the Peeling Skin Disease," *American Journal of Human Genetics* 87 (2010): 274–281, https://doi.org/10.1016/j.ajhg.2010.07.005.

53. B. Kalb, I. Marenholz, A. C. S. N. Jeanrenaud, et al., "Filaggrin Loss-Of-Function Mutations Are Associated With Persistence of Egg and Milk Allergy," *Journal of Allergy and Clinical Immunology* 150 (2022): 1125–1134, https://doi.org/10.1016/j.jaci.2022.05.018.

54. D. D. Bikle, "Vitamin D Metabolism, Mechanism of Action, and Clinical Applications," *Chemistry & Biology* 21 (2014): 319–329, https://doi.org/10.1016/j.chembiol.2013.12.016.

55. K. R. Aass, M. H. Kastnes, and T. Standal, "Molecular Interactions and Functions of IL-32," *Journal of Leukocyte Biology* 109 (2021): 143–159, https://doi.org/10.1002/JLB.3MR0620-550R.

56. E. Psaroulaki, G. N. Katsaras, P. Samartzi, et al., "Association of Food Allergy in Children With Vitamin D Insufficiency: A Systematic Review and Meta-Analysis," *European Journal of Pediatrics* 182 (2023): 1533–1554, https://doi.org/10.1007/s00431-023-04843-2.

57. E. Hyppönen, U. Sovio, M. Wjst, et al., "Infant Vitamin d Supplementation and Allergic Conditions in Adulthood: Northern Finland Birth Cohort 1966," *Annals of the New York Academy of Sciences* 1037 (2004): 84–95, https://doi.org/10.1196/annals.1337.013.

58. M. Wjst, "Another Explanation for the Low Allergy Rate in the Rural Alpine Foothills," *Clinical and Molecular Allergy* 3 (2005): 7, https://doi.org/10.1186/1476-7961-3-7.

59. C. Norizoe, N. Akiyama, T. Segawa, et al., "Increased Food Allergy and Vitamin D: Randomized, Double-Blind, Placebo-Controlled Trial," *Pediatrics International* 56 (2014): 6–12, https://doi.org/10.1111/ped.12207.

60. J. Rosendahl, A. S. Pelkonen, O. Helve, et al., "High-Dose Vitamin D Supplementation Does Not Prevent Allergic Sensitization of Infants," *Journal of Pediatrics* 209 (2019): 139–145.e1, https://doi.org/10.1016/j.jpeds.2019.02.021.

61. E. Hyppönen, D. J. Berry, M. Wjst, and C. Power, "Serum 25-Hydroxyvitamin D and IgE—A Significant but Nonlinear Relationship," *Allergy* 64 (2009): 613–620, https://doi.org/10.1111/j.1398-9995.2008.01865.x.

62. D. Chauss, T. Freiwald, R. McGregor, et al., "Autocrine Vitamin D Signaling Switches Off Pro-Inflammatory Programs of TH1 Cells," *Nature Immunology* 23 (2022): 62–74, https://doi.org/10.1038/s41590-021-01080-3.

63. S. Imran, M. R. Neeland, J. Koplin, et al., "Epigenetic Programming Underpins B-Cell Dysfunction in Peanut and Multi-Food Allergy," *Clinical & Translational Immunology* 10 (2021): e1324, https://doi.org/10.1002/cti2.1324.

64. A. N. Do, C. T. Watson, A. T. Cohain, et al., "Dual Transcriptomic and Epigenomic Study of Reaction Severity in Peanut-Allergic Children," *Journal of Allergy and Clinical Immunology* 145 (2020): 1219–1230, https://doi.org/10.1016/j.jaci.2019.10.040.

65. D. Martino, J. E. Joo, A. Sexton-Oates, et al., "Epigenome-Wide Association Study Reveals Longitudinally Stable DNA Methylation Differences in CD4+ T Cells From Children With IgE-Mediated Food Allergy," *Epigenetics* 9 (2014): 998–1006, https://doi.org/10.4161/epi.28945.

66. Z. Zhu, Y. Guo, H. Shi, et al., "Shared Genetic and Experimental Links Between Obesity-Related Traits and Asthma Subtypes in UK Biobank," *Journal of Allergy and Clinical Immunology* 145 (2020): 537–549, https://doi.org/10.1016/j.jaci.2019.09.035.

67. M. Oliva, M. K. Sarkar, M. E. March, et al., "Integration of GWAS, QTLs and Keratinocyte Functional Assays Reveals Molecular Mechanisms of Atopic Dermatitis," *Nature Communications* 16 (2025): 3101, https://doi.org/10.1038/s41467-025-58310-7.

68. S. Ahmad, N. A. Azid, J. C. Boer, et al., "The Key Role of TNF-TNFR2 Interactions in the Modulation of Allergic Inflammation: A Review," *Frontiers in Immunology* 9 (2018): 2572, https://doi.org/10.3389/fimmu.2018.02572.

69. D. A. A. Vignali and V. K. Kuchroo, "IL-12 Family Cytokines: Immunological Playmakers," *Nature Immunology* 13 (2012): 722–728, https://doi.org/10.1038/ni.2366.

70. G. Trinchieri, "Interleukin-12: A Cytokine Produced by Antigen-Presenting Cells With Immunoregulatory Functions in the Generation of T-Helper Cells Type 1 and Cytotoxic Lymphocytes," *Blood* 84 (1994): 4008–4027.

71. E. D. Tait Wojno, C. A. Hunter, and J. S. Stumhofer, "The Immunobiology of the Interleukin-12 Family: Room for Discovery," *Immunity* 50 (2019): 851–870, https://doi.org/10.1016/j.immuni.2019.03.011.

72. M. Hoshino, Y. Nakamura, and Q. A. Hamid, "Gene Expression of Vascular Endothelial Growth Factor and Its Receptors and Angiogenesis in Bronchial Asthma," *Journal of Allergy and Clinical Immunology* 107 (2001): 1034–1038, https://doi.org/10.1067/mai.2001.115626.

73. N. Meyer and C. A. Akdis, "Vascular Endothelial Growth Factor as a Key Inducer of Angiogenesis in the Asthmatic Airways," *Current Allergy and Asthma Reports* 13 (2013): 1–9, https://doi.org/10.1007/s11882-012-0317-9.

Supporting Information

Additional supporting information can be found online in the Supporting Information section. **Figure E1.** Overview of the cohort and samples, estimated cell composition, association analysis of age and OFC eliciting dose, and case–control methylation DMR and genomic inflation data (a) Flow diagram illustrating differences between "individual" and "sample" numbers during the workflow. The asterisk indicates a loss of two samples due to low cell number after thawing. In such cases, the stimulated cell culture conditions were prioritized and there were fewer quiescent samples. (b) Estimated cell composition using DNA methylation data. Significance determined by a Wilcoxon rank-sum test between hazelnut allergic and nonallergic groups is denoted by asterisks ($p < 0.05$). (c) Relationship between age and the maximum tolerated dose during OFC in the allergic cohort. Age was stratified into tertiles. For plotting and statistical purposes, the maximum tolerated dose was converted to a logarithmic scale (log10). Doses of 0 grams were offset to 0.001 g to allow for successful conversion. (d) Number of DMRs detected in each analysis. Overlapping DMRs not show. (e) Quantile-quantile (QQ) plot showing the observed versus expected *p*-values of the DNA methylation analysis for the quiescent (left) and stimulated (right) probes. DMR, differentially methylated region; OFC, oral food challenge; QC, quality control. **Figure E2.** Summary of gene expression case–control data. (a) Heatmap of averaged z- scores showing the genes most highly differentiating between allergic and nonallergic individuals. (b) GOplot highlighting the key driver terms in the GO:MF analysis category using significant genes after hazelnut stimulation. The effect direction of each gene is highlighted. The GOplot *Z*-score indicates the balance of up versus downregulated genes contributing to each term. (c) Genes contributing to the JAK–STAT signalling pathway (* = $p < 0.05$, ** = $p < 0.01$). (d) GSEA analysis of hallmark gene sets generated from genes in the case–control stimulated samples. BP, biological processes; GO, gene ontology; GSEA, Gene Set Enrichment Analysis; MF, molecular function. **Figure E3.** Altered protein expression in hazelnut allergy. (a) Volcano plot highlighting the five differentially secreted proteins between hazelnut allergic and nonallergic individuals in response to stimulation. (b) Violin plots showing the distributions of each protein. All proteins are significantly more secreted in allergic individuals in response to hazelnut stimulation compared to the nonallergic individuals ($p < 0.05$). **Table E1.** Overview of packages used in the computational analysis of this study. Package names as well as versions and maintainers are shown. **Table E2.** Summary of the wet-lab reagents used in this study with company and catalogue numbers, where relevant. **Table E3.** Characteristics of the hazelnut cohort and nonallergic controls. Parameters include self-reported ethnicity and cell type proportion estimates. The demographic data is presented as the number and percentage of participants in each category. The cell type estimates are presented as median and quartiles (Q1, Q3). The *p*-value is calculated by Pearson's Chi-squared test1 or Wilcoxon rank sum test2. **Table E4.** Summary of examined statistical models and comparisons. For the DNA methylation and Protein analysis, Limma was used while DESeq2 was used for gene expression analysis. †Cell composition: CD4 T cell + CD8 T cell + B cell + monocyte + natural killer cell type proportions based on estimations from DNA methylation. **Table E5.** Summary statistics and information of DNA methylation probe data in this study. Only significant DMP or DMR data were retained. "Chromosome", "Start", and "End" describe the CpG hg38 coordinates. "Probe_ID" is the unique identifier for each probe. "Overlapping genes" describes the names of genes associated with the probe. "Transcript types" is the type of transcript of the associated probe gene. Remaining columns show the effect size (logFC) and nominal *p*-values (*p*-value) from various analyses. **Table E6.** List of significant DMRs in the case-control quiescent and hazelnut analyses. DMR coordinates are shown along with the average log fold change (LogFCμ). The direction, width, adjusted *p*-value, and number of probes for each DMR are also shown. The probe IDs for each DMR are listed. The genes associated (overlapping unless otherwise stated) with each DMR are listed as well as the case-control analysis in which the DMR was detected. DMRs are ordered by *p*-value within each analysis. **Table E7.** List of significant DMRs in the case-control quiescent and hazelnut analyses comparing the main analysis (blue) with a sensitivity analysis excluding individuals of non-European ancestry (green). Only overlapping (full or partial) DMRs are compared against the original analysis. Newly detected DMRs in the European-only analyse are not shown. DMR coordinates are shown. The adjusted *p*-value, and number of probes for each DMR are also shown. The probe IDs for each DMR are listed. The analysis type column shows in which of the case-control analyses the DMR was detected. The genes associated (overlapping) with each DMR are listed. In cases where the structure of the DMRs do not match identically between analyses, an asterisk (*) is denoted in the "Analysis type" column. Double asterisks (**) indicate reported signals that are no longer detected when performing the sensitivity analysis. These signals should

be interpreted with caution. DMRs are ordered by *p*-value of the main analysis and within each analysis type. **Table E8.** Summary statistics of gene expression data in this study. Data is split into summary statistics for three analyses. "Gene name/Ensembl ID" is the gene symbol or, if no symbol is present, the Ensembl ID of this gene. If multiple gene symbols mapped to the same ID, the strings were concatenated. "baseMean" describes the average expression of a gene across analyses. Columns showing the effect size (logFC/log2 fold change), the nominal *p*-value (*p*-nom), and FDR-corrected *p*-value (*p*-FDR) of various analyses are shown. "Case control Quiescent" (blue) and "case control Stimulated" (green) are the results of the case–control analysis for quiescent or stimulated samples, respectively. "interaction" (grey) columns show the results of the interaction analysis. For each analysis, genes in each analysis are ranked independantly by significance (increasing adjusted *p*-value and priority of genes with absolute logFC over 0.3). Signficant genes are highlighted. **Table E9.** Functional enrichment results of differentially expressed case–control genes post-antigen stimulation. The GO term, FDR-corrected *p*-value, term size, term-query intersection size, source, and list of genes making up the term are shown. These results show the terms passing QC thresholds described in the methodology for GO, KEGG, and Reactome (REAC) pathways. Terms are ranked by *p*-value, regardless of group. BP, biological processes; CC, cellular component; GO, gene ontology; MF, molecular function. **Table E10.** Summary statistics of protein expression data in this study. Both the protein and gene names are shown. Columns showing the effect size (logFC/log2 fold change), nominal *p*-value (*p*-nom), and FDR-corrected *p*-value (*p*-FDR) of various analyses are shown. "Case control Quiescent" (blue) and "case control Stimulated" (green) are the results of the case–control analysis for quiescent or stimulated samples, respectively. "Interaction" (grey) columns are the results of the interaction analysis. A binary filter for significant genes in the interaction without logFC filter is given ("Interaction protein"). For each analysis, genes are ranked independantly by adjusted *p*-value. **Table E11.** Functional enrichment results from differentially expressed case-control proteins after stimulation. The GO term, FDR-corrected *p*-value, term size, term-query intersection size, source, and list of genes making up the term are shown. No GO terms were detected in this analysis. **Table E12.** DMR-DEG overlaps shown with the corresponding group, chromosome, start and end hg38 coordinates, DMR width (bp), Pearson correlation coefficient, adjusted *p*-value, and absolute distance from the middle of the DMR to the TSS of the corresponding gene (bp). A test of correlation differences between groups is also shown (Pr.test). Data is from hazlnut-stimulated samples. **Table E13.** Multi-omics factor analysis weightings for each feature. Shown are the features (gene names; underscored by the omics layer or Probe ID). Where more than one gene are associated per row (in the case of methylation probes), genes are also shown in wide format (Gene 1–10). Latent factors associated with phenotypes are shown. Weightings and absolute weightings for each feature are shown. The relevant omics layers are shown. Data is sorted by Latent factor, then absolute weight. **Table E14.** Multi-omics factor analysis enrichr analysis results. Significant gene FDR-adjusted *p* value threshold of 0.05 and overlapping query genes of at least 10. Results are shown for GO biological processes, Reactome, and KEGG databases. The number of query overlap genes are shown as well as the odds ratio and genes contributing to the each set. Sets are ranked by adjusted *p*-value within each factor and database. **Data S1:** all70525-sup-0005-Supinfo5.docx.